

Artificial Neural Network for Optimizing Gamma Radiation Shielding

Mahdieh Mokhtari Dorostkar (PhD Candidate)¹, Fatemeh Sadat Rasouli (PhD)^{2*}

¹Department of Physics, Urmia University, Urmia, Iran

²Department of Physics, K.N. Toosi University of Technology, Tehran, Iran

ABSTRACT

Background: Designing shields for gamma radiation sources is particularly important due to their extensive use in medical, industrial, and research studies.

Objective: This study aimed to explore the ability of an Artificial Neural Network (ANN) to identify the optimized shield for a typical gamma source. Despite the effectiveness of Monte Carlo simulations in determining optimal shielding materials and geometries, they are time-consuming and require numerous simulations for each configuration.

Material and Methods: In this simulating study, the MCNPX Monte Carlo code was utilized to conduct simulations using a previously proposed shielding material. After validating the simulation accuracy, a large dataset was generated to serve as input and target data for the machine learning process. The method's precision was assessed by comparing the results of the ANN with those of Monte Carlo simulations. Dose calculations were performed using a water phantom.

Results: The deviation of less than 1% was computed between the simulation and the ANN. The network also exhibited satisfactory predictions for unknown data. Additionally, the dose was evaluated using a water phantom to assess further and optimize the selected shielding material.

Conclusion: The ANNs are widespread and significant in radiation shielding studies. The developed network can accurately predict unknown weight fraction combinations. The designed network can effectively predict unknown weight fraction combinations.

Keywords

Monte Carlo Method; Dose; Gamma Radiation; Shielding; Phantom; Machine Learning; Computer Simulation; Exposure

Introduction

Reducing personal exposure by improving shielding properties is an important subject in radiation safety [1]. Single or mixed radiation sources have been provided due to the increasing growth of nuclear energy in various aspects of technology, medicine, diagnostics, and imaging, and have made radiation shielding an interesting subject for research in physics and nuclear engineering [2].

Various materials can be considered based on the type and intensity of the source and application of the shield. For gamma rays, which the present work deals with, these shields can include concretes, alloys, glasses, and epoxy-based composite shields [3-10]. Among these materials,

*Corresponding author:
Fatemeh Sadat Rasouli
Department of Physics,
K.N. Toosi University of
Technology, Tehran, Iran
E-mail:
rasouli@kntu.ac.ir

Received: 9 October 2023
Accepted: 3 August 2024

glasses are widely used for radiation protection because they serve dual functions: being transparent to visible light while also absorbing gamma rays and neutrons. Additionally, their composition can include a diverse range of elements, making them a versatile shield that researchers can tailor to their needs [2]. Heavy metal oxide glasses, including silicate, and borate glasses have been confirmed to have excellent potential as shielding materials. Tellurite glasses have recently gained interest due to their low melting point, high thermal ability, low crystallization, proper chemical resistance, and high dielectric constant [11-13]. These glasses are recommended for use in medicine and photonics, including laser production, optical amplifiers, aerial surveillance equipment, and various other devices [14].

There are two possible approaches for the design and optimization of shields, including the analytical method and Monte Carlo simulations. Monte Carlo is a well-known method for not only studying particle transport and possible interactions through the medium but also simulating complicated geometries and multi-layer materials. However, the accuracy of the Monte Carlo method is essentially based on repeated random sampling and a number of transported histories. Accordingly, the examination is time-consuming. Artificial Neural Networks (ANNs) provide a series of algorithms to recognize a relationship between a set of input data through a process inspired

by the human brain and to prevent researchers from doing time-consuming simulations or experiments for all available situations in the problem under consideration. The ANN is a shortcut to save time and cost of computational methods by using a limited number of simulations or experimental data.

The present work is devoted to studying the feasibility of using ANN to analyze and optimize the shield for radiation sources. To this aim, a glass gamma shield ($\text{TeO}_2\text{-V}_2\text{O}_5\text{-Bi}_2\text{O}_3$) was simulated for a 2.056 MeV gamma-ray source [5]. By considering different variables, such as the weight fraction of the compositions, a set of Monte Carlo input data was extracted for learning ANNs. The results were tested by surveying the accuracy of the method. MCNPX code (version 2.6) was utilized for simulations and transport of the particles.

Material and Methods

Monte Carlo simulations

In this simulating study, based on the referenced shield proposed by Hendi et al. [5], 3 cm of the $\text{TeO}_2\text{-V}_2\text{O}_5\text{-Bi}_2\text{O}_3$ glass was considered. There was a gamma collimator made of lead with an outer radius of 11.35 cm and an inner radius of 1.5 mm, surrounding the gamma source of 2.056 MeV and the HPGe detector. The gamma source was located at a distance of 9 cm from the sample. Figure 1 shows a

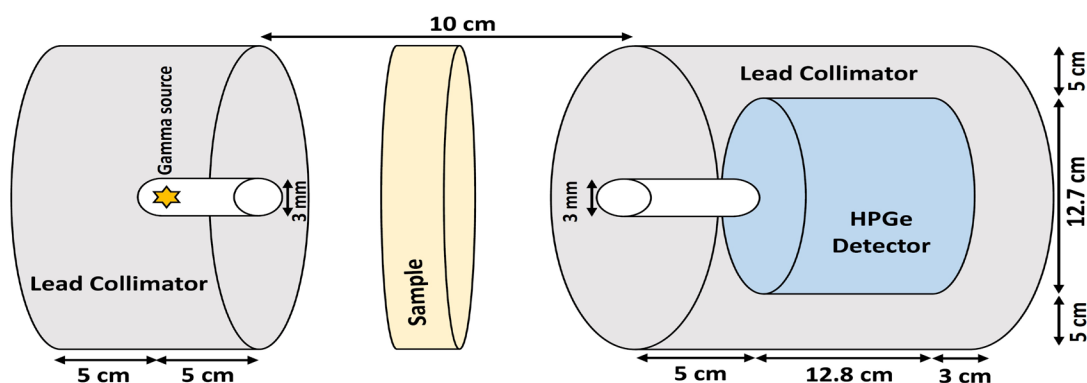


Figure 1: A schematic view of the simulated geometry, components, and dimensions based on the work proposed by Hendi et al [5].

schematic view of the simulated geometry.

Providing data for machine learning

As the prominent data processing systems, ANNs can provide intelligent relations, linear, and non-linear, between the input and output data. The modeling consists of a network of nonlinear information that processes the initial input information. These are normally arranged in layers and executed in parallel, known as the topology of a neural network. These nonlinear information processing elements in the network are called neurons with interconnections named synaptic weights. The learning algorithm is vital in training the network to analyze the input data in a meaningful way. Neural networks are trained with supervised algorithms, in which the desired output must be provided for the corresponding input data set employed in the training of the machine [15]. By increasing the amount of entrance information, the accuracy of the calculations is expected to increase. The input data may be generated by taking into account multiple parameters by using either simulations or experimental works. In the present study, various parameters are available, such as the shield thickness, the elements of

compositions, source energy, and source particle type.

Figure 2 is a schematic view of a simple network process and the three types of constructing layers. The input layer is the data given to the machine as available information, processed through the hidden layer(s). In the next step, another data is provided by the output layer, which is the output data set.

The weight fractions of the elements in the glass compounds were treated as variable parameters. These fractions were adjusted from 2% to 96% for each component in increments of 2%. Equation (1) was used to calculate these weight fractions, as follows:

$$wf(x_i) = \frac{w_i}{100} \cdot \frac{N \times M_{x_i}}{M_i} \quad (1)$$

where w_i is the percentage of the presence of the i^{th} element, N is the number of the element in the compound, M_{x_i} is the molecular weight of the i^{th} element, and M_i is the molecular weight of the compound.

Utilizing the mentioned geometry (Figure 1), simulations have been accomplished by using MCNPX code for five weight fractions reported in Figure 3, and also the accuracy of the simulation has been approved by comparing the obtained results with those

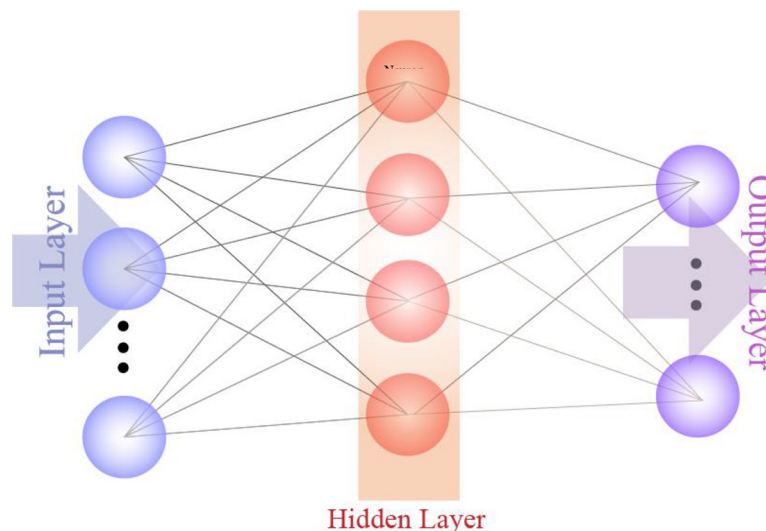


Figure 2: A schematic view of the neural network process.

of Hendi et al., [5].

Changing the weight fractions results in 900 MCNPX samples, which provides an appropriate input matrix for machine learning. Table 1 reports examples of the calculated weight fractions in 900 samples with the step of 100 in their labeled number.

The number of photons on the arrival window of the HPGe detector has been

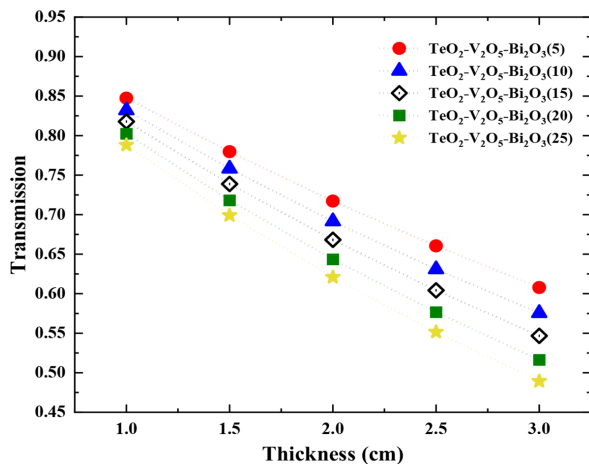


Figure 3: The transition of the gamma rays versus the thickness for various weight fractions suggested by Hendi et al., [5].

counted using the F1 tally. Hence, two datasets were used for the input and target of the network: a 4×900 matrix that constitutes the input matrix, and a 1×900 matrix that forms the target matrix. After generating the input and the target matrix, the neural network analyzes the data.

The designed neural network predicts particle counts for provided samples in the detector after passing through a TeO₂-V₂O₅-Bi₂O₃ glass; the neural network processes the input matrix and finds the relation between the input and the target matrixes by changing the weight in its function. The designed model was developed using the Feed-Forward Back Propagation Network type with the adoption learning function of the Levenberg-Marquardt algorithm and calculating mean square error. For the given dataset, 25 neurons and one hidden layer were obtained as optimized structures. Figure 4 represents a schematic view of the designed network.

Dose evaluations

The efficiency of the optimized sample was investigated through the physical dose for different thicknesses. In this calculation, a wa-

Table 1: Examples of weight fraction calculations for the TeO₂-V₂O₅-Bi₂O₃ glass.

| No. | TeO ₂ -V ₂ O ₅ -Bi ₂ O ₃ | | | | | | |
|-----|---|-------------------------------|--------------------------------|--------------------------|----------|-----------|---------|
| | Component (%) | | | Elements weight fraction | | | |
| | TeO ₂ | V ₂ O ₅ | Bi ₂ O ₃ | Oxygen | Vanadium | Tellurium | Bismuth |
| 50 | 0.04 | 0.04 | 0.92 | 0.121 | 0.022 | 0.032 | 0.825 |
| 100 | 0.06 | 0.1 | 0.84 | 0.143 | 0.056 | 0.048 | 0.754 |
| 200 | 0.1 | 0.28 | 0.62 | 0.207 | 0.157 | 0.080 | 0.556 |
| 300 | 0.14 | 0.54 | 0.32 | 0.299 | 0.303 | 0.112 | 0.287 |
| 400 | 0.2 | 0.08 | 0.72 | 0.150 | 0.045 | 0.159 | 0.646 |
| 500 | 0.24 | 0.54 | 0.22 | 0.309 | 0.303 | 0.191 | 0.197 |
| 600 | 0.3 | 0.38 | 0.32 | 0.261 | 0.213 | 0.239 | 0.287 |
| 700 | 0.36 | 0.4 | 0.24 | 0.274 | 0.224 | 0.287 | 0.215 |
| 800 | 0.44 | 0.04 | 0.52 | 0.161 | 0.022 | 0.351 | 0.466 |
| 900 | 0.5 | 0.48 | 0.02 | 0.314 | 0.269 | 0.399 | 0.018 |

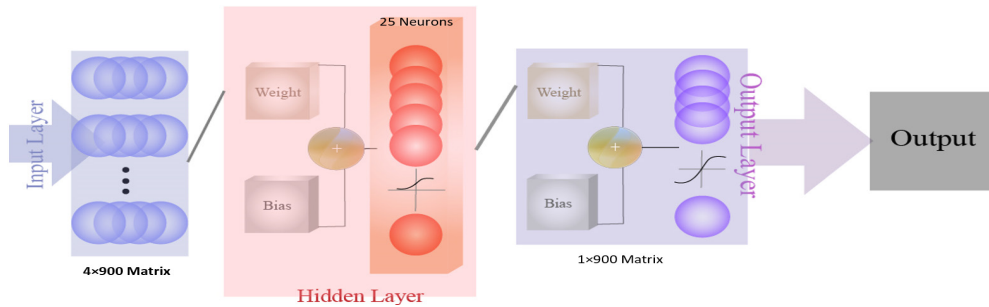


Figure 4: The neural network process used in the present work.

ter-filled phantom was located in the detector position (Figure 1). Tally F6 has been used for dose calculations with a relative error of less than 1%.

Results

Training by all the data

At first, the learning precision of the network has been investigated for all data. In this step, the network has been evaluated with all samples of the input data. Hence, the 4×900 input matrix was given to the network as input and the 1×900 matrix was considered as the target. The network has been trained with the given information. Figure 5 illustrates the results of this training.

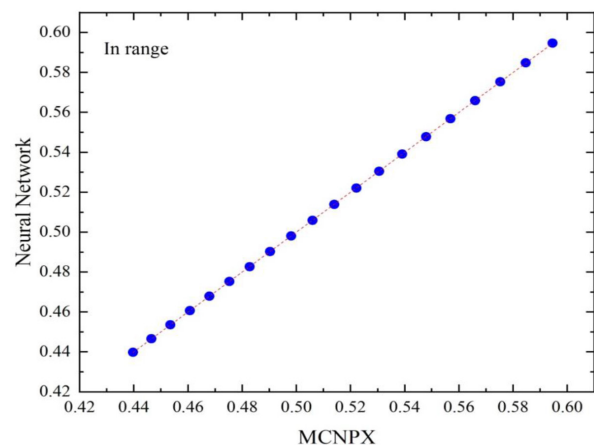


Figure 5: Comparison of the results obtained through Artificial Neural Network (ANN) by training all 900 data with those of MCNPX code.

Training more than 98% of the data

The input matrix was considered up to 880th samples, in which the matrix will be 4×880 , and the target matrix will be 1×880 . The network was trained for these samples and was asked to estimate the 20 remained data. Figure 6 presents the network performance compared to the MCNP results for the F1 tally.

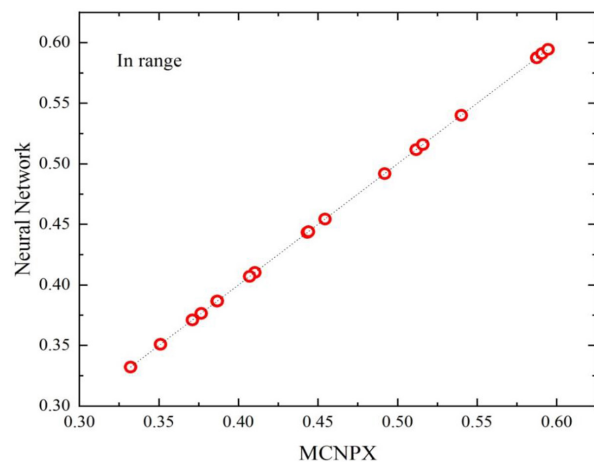


Figure 6: Comparison of the results of the last 20 data in the MCNPX input data set with those of ANN.

ral network. In the next step, the network was supposed to predict the new unknown samples, i.e. are out of range. Table 2 represents a comparison between the results predicted by the network and those of the MCNPX simulations.

Optimizing dimension

In this part, the weight fraction of the sample labeled as number 399, showing that the best performance has been selected for thickness optimization. Thicknesses of 1 to 8 cm were candidates as radiation shields. In addition, dose evaluation was considered for these samples. Figure 7 reports the results of this investigation by considering the activity of 20 μ Ci for the gamma source.

Discussion

As shown in Figure 5, the predicted F1 tally by ANN is in acceptable agreement with those of the MCNPX results. The deviation between ANN and MCNPX results was less than 1%. Therefore, the trained network has the capability for the prediction of unknown weight fractions to evaluate outputs. Also, Figure 6 shows acceptable agreement between the results of 20 points of MCNPX input data with those of ANN. According to the data presented in Table 2, the ANN has also appropriate performance for unknown samples that were not trained before. In Figure 7, the calculated dose in the water phantom was examined for various thicknesses of the sample. IAEA recommended dose limits for workers per year and compared the results of Figure 7 with the whole-body dose limit of 1 mSv per year.

Conclusion

This study is focused on a particular glass shield as an example. First, the accuracy of the simulation was checked with the referenced shield results. Next, a great dataset was gathered through the simulations accomplished using MCNPX2.6 code. Then, this dataset was used to form input and target matrices

in MATLAB. Also, there was a comparison between the results from the simulation and the network. Finally, the samples which the corresponding data were not learned to the machine before, were used to assess the ANN performance. The results were compared with those of the simulations.

Table 2: The results of the neural network for completely unknown samples. In addition, MCNPX results were used to investigate the validation of ANN results.

| NO. | MCNPX | Neural Network | Error (%) |
|-----|-------|----------------|-----------|
| 1 | 0.335 | 0.328 | 2 |
| 2 | 0.364 | 0.357 | 1.9 |
| 3 | 0.589 | 0.586 | 0.5 |
| 4 | 0.371 | 0.363 | 2.1 |
| 5 | 0.529 | 0.524 | 0.9 |
| 6 | 0.419 | 0.412 | 1.7 |
| 7 | 0.481 | 0.474 | 1.4 |
| 8 | 0.477 | 0.470 | 1.4 |
| 9 | 0.420 | 0.413 | 1.6 |
| 10 | 0.496 | 0.490 | 1.2 |

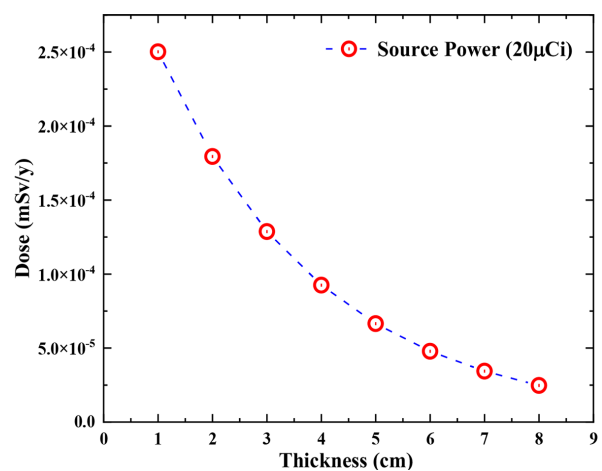


Figure 7: Comparison of dose results and dose limitation.

There is a significant correlation between the results of the considered network and simulation. The deviation was less than 1% in data set comparisons and unknown samples. Therefore, this method can be a simple and affordable way to design the appropriate shield without using Monte Carlo simulations.

This study is focused on a particular glass shield as an example. First, the accuracy of the simulation was checked with the referenced shield results. Next, a great dataset was gathered through the simulations accomplished using MCNPX2.6 code. Then, this dataset was used to form input and target matrices in MATLAB. Also, there was a comparison between the results from the simulation and the network. Finally, the samples which the corresponding data were not learned to the machine before, were used to assess the ANN performance. The results were compared with those of the simulations.

There is a significant correlation between the results of the considered network and simulation. The deviation was less than 1% in data set comparisons and unknown samples. Therefore, this method can be a simple and affordable way to design the appropriate shield without using Monte Carlo simulations.

The dose was evaluated in the case of the optimized weight fraction for 20 μCi source intensity. In addition, considering the annual dose limitation of 1 mSv for individuals, it was tried to find the optimized dimension for the sample to decrease the dose. For this purpose, 8 samples with thicknesses of 1 to 8 cm with steps of 1 cm were tested.

The trained network not only leads to acceptable results in a known dataset of given input and target but also is used for unknown samples out of the range of the training dataset. In addition, the network precision was considered with some randomly unknown samples. The deviation between the predicted results from those of the MCNPX simulations was less than 2%. The results emphasize that the final optimum shield can be obtained based

on the prepared dataset without conventional calculations based on the MCNPX code. It is worth mentioning that the present results can be extended to the simulation of more complicated models of the arrangement of the source, the shield, and the detector considering a wide span of shield materials. Also, it can be investigated for other sources or mixed radiation fields. The present results are encouraging and the mentioned problems offer new ways to accomplish more research on the performance of the ANN in optimization studies.

Authors' Contribution

All authors conceived the project, prepared the data and figures, and analyzed the results. Both authors wrote and reviewed the main manuscript text and approved the final version.

Ethical Approval

This is a simulation study. No ethical approval is required.

Funding

This research received no specific grant from any funding agency in the public, commercial, or not-for-profit sectors.

Conflict of Interest

None

References

1. McAlister DR. Gamma ray attenuation properties of common shielding materials. USA: University Lane Lisle; 2012.
2. Manohara SR, Hanagodimath SM, Gerward L. Photon interaction and energy absorption in glass: a transparent gamma ray shield. *Journal of Nuclear Materials*. 2009;**393**(3):465-72. doi: 10.1016/j.jnucmat.2009.07.001.
3. Gaikwad DK, Sayyed MI, Obaid SS, Issa SA, Pawar PP. Gamma ray shielding properties of TeO₂-ZnF₂-As₂O₃-Sm₂O₃ glasses. *Journal of Alloys and Compounds*. 2018;**765**:451-8. doi: 10.1016/j.jallcom.2018.06.240.
4. Kumar A, Gaikwad DK, Obaid SS, Tekin HO, Agar O, Sayyed MI. Experimental studies and Monte Carlo simulations on gamma ray shield-

- ing competence of $(30+x)$ PbO₁₀WO₃ 10Na₂O–10MgO–(40-x) B₂O₃ glasses. *Progress in Nuclear Energy*. 2020;**119**:103047. doi: 10.1016/j.pnucene.2019.103047.
5. Hendi AA, Rashad M, Sayyed MI. Gamma radiation shielding study of tellurite glasses containing V₂O₅ and Bi₂O₃ using Geant4 code. *Ceramics International*. 2020;**46**(18):28870-6. doi: 10.1016/j.ceramint.2020.08.053.
 6. Kaur S, Kaur A, Singh PS, Singh T. Scope of Pb-Sn binary alloys as gamma rays shielding material. *Progress in Nuclear Energy*. 2016;**93**:277-86. doi: 10.1016/j.pnucene.2016.08.022.
 7. Singh VP, Badiger NM. Gamma ray and neutron shielding properties of some alloy materials. *Annals of Nuclear Energy*. 2014;**64**:301-10. doi: 10.1016/j.anucene.2013.10.003.
 8. Canel A, Korkut H, Korkut T. Improving neutron and gamma flexible shielding by adding medium-heavy metal powder to epoxy based composite materials. *Radiation Physics and Chemistry*. 2019;**158**:13-6. doi: 10.1016/j.radphyschem.2019.01.005.
 9. El-Khatib AM, Doma AS, Badawi MS, Abu-Rayan AE, Aly NS, Alzahrani JS, Abbas MI. Conductive natural and waste rubbers composites-loaded with lead powder as environmental flexible gamma radiation shielding material. *Materials Research Express*. 2020;**7**(10):105309. doi: 10.1088/2053-1591/abbf9f.
 10. Kim SC, Son JS. Double-layered fiber for light-weight flexible clothing providing shielding from low-dose natural radiation. *Scientific Reports*. 2021;**11**(1):3676. doi: 10.1038/s41598-021-83272-3.
 11. El-Mallawany R. Evaluation of optical parameters of some tellurite glasses. *Optik*. 2014;**125**(20):6344-6. doi: 10.1016/j.ijleo.2014.07.129.
 12. El-Mallawany R, Sayyed MI. Comparative shielding properties of some tellurite glasses: Part 1. *Physica B: Condensed Matter*. 2018;**539**:133-40. doi: 10.1016/j.physb.2017.05.021.
 13. El-Mallawany R, Ahmed IA. Thermal properties of multicomponent tellurite glass. *J Mater Sci*. 2008;**43**(15):5131-8. doi: 10.1007/s10853-008-2737-4.
 14. Al-Hadeethi Y, Sayyed MI. Radiation attenuation properties of Bi₂O₃–Na₂O–V₂O₅–TiO₂–TeO₂ glass system using Phy-X/PSD software. *Ceramics International*. 2020;**46**(4):4795-800. doi: 10.1016/j.ceramint.2019.10.212.
 15. Mander L, Liu HW. Comprehensive natural products II: chemistry and biology. Elsevier; 2010.